Modulation of hypothalamic AMPK phosphorylation by olanzapine controls energy balance and body weight

Vitor Ferreira [a,b], Cintia Folgueira [c], Maria Guillén [a], Pablo Zubiaur [d,e], Marcos Navares [e], Assel Sarsenbayeva [f], Pilar López-Larrubia [a], Jan W. Eriksson [f], Maria J. Pereira [f], Francisco Abad-Santos [d,e,g], Guadalupe Sabio [c], Patricia Rada [a,b,*], Ángela M. Valverde [a,b,*]

[a] Instituto de Investigaciones Biomedicas Alberto Sols (IIBM), CSIC-UAM, Madrid, Spain
[b] Centro de Investigación Biomédica en Red de Diabetes y Enfermedades Metabólicas Asociadas (CIBERdem), ISCIII, Spain
[c] Centro Nacional de Investigaciones Cardiovasculares (CNIC), 28029 Madrid, Spain
[d] Clinical Pharmacology Department, School of Medicine, Hospital Universitario de La Princesa, Instituto Teófilo Hernando, Universidad Autónoma de Madrid, Instituto de Investigación Sanitaria La Princesa (IP), Madrid, Spain
[e] UICEC Hospital Universitario de La Princesa, Platform SCReN (Spanish Clinical Research Network), Instituto de Investigación Sanitaria La Princesa (IP), Madrid, Spain
[f] Department of Medical Sciences, Clinical Diabetes and Metabolism, Uppsala University, Uppsala, Sweden
[g] Centro de Investigación Biomédica en Red de Enfermedades Hepáticas y Digestivas (CIBERehd), Instituto de Salud Carlos III, Madrid, Spain

ARTICLE INFO

ABSTRACT

Background: Second-generation antipsychotics (SGAs) are a mainstay therapy for schizophrenia. SGA-treated patients present higher risk for weight gain, dyslipidemia and hyperglycemia. Herein, we evaluated the effects of olanzapine (OLA), widely prescribed SGA, in mice focusing on changes in body weight and energy balance. We further explored OLA effects in protein tyrosine phosphatase-1B deficient (PTP1B-KO) mice, a preclinical model of leptin hypersensitivity protected against obesity.

Methods: Wild-type (WT) and PTP1B-KO mice were fed an OLA-supplemented diet (5 mg/kg/day, 7 months) or treated with OLA via intraperitoneal (i.p.) injection or by oral gavage (10 mg/kg/day, 8 weeks). Readouts of the crosstalk between hypothalamus and brown or subcutaneous white adipose tissue (BAT and iWAT, respectively) were assessed. The effects of intrahypothalamic administration of OLA with adenoviruses expressing constitutive active AMPKα1 in mice were also analyzed.

Results: Both WT and PTP1B-KO mice receiving OLA-supplemented diet presented hyperphagia, but weight gain was enhanced only in WT mice. Unexpectedly, all mice receiving OLA via i.p. lost weight without changes in food intake, but with increased energy expenditure (EE). In these mice, reduced hypothalamic AMPK phosphorylation concurred with elevations in UCP-1 and temperature in BAT. These effects were also found by intrahypothalamic OLA injection and were abolished by constitutive activation of AMPK in the hypothalamus. Additionally, OLA i.p. treatment was associated with enhanced Tyrosine Hydroxylase (TH)-positive innervation and less sympathetic neuron-associated macrophages in iWAT. Both central and i.p. OLA injections increased UCP-1 and TH in iWAT, an effect also prevented by hypothalamic AMPK activation. By contrast, in mice fed an OLA-supplemented diet, BAT thermogenesis was only enhanced in those lacking PTP1B. Our results shed light for the first time that a threshold of OLA levels reaching the hypothalamus is required to activate the hypothalamus BAT/iWAT axis and, therefore, avoid weight gain.

Conclusion: Our results have unraveled an unexpected metabolic rewiring controlled by hypothalamic AMPK that avoids weight gain in male mice treated i.p. with OLA by activating BAT thermogenesis and iWAT browning and a potential benefit of PTP1B inhibition against OLA-induced weight gain upon oral treatment.

1. Introduction

Schizophrenia is a chronic severe psychiatric disorder that appears in late adolescence/early adulthood [1]. According to current clinical guidelines, the second-generation (atypical) antipsychotic (SGA) drugs constitute the mainstay treatment for schizophrenia and other psychiatric disorders [2]. Due to the exponential risk of relapse when the treatments are discontinued, patients undergo life-long treatments with the SGA initially prescribed in the acute phase for as long as it is effective and well-tolerated. Compared to first-generation antipsychotics (FGAs), SGAs have superior therapeutic effects and lower probability of causing extrapyramidal symptoms. However, clinical observations revealed several metabolic alterations in patients under SGA treatment, such as body weight gain, hyperglycemia, and dyslipidemia [3,4]. In fact, patients with schizophrenia have a three-fold higher risk of developing obesity and two to four-fold higher risk of type 2 diabetes mellitus (T2D) [5]. The role of SGAs in the development of metabolic complications was supported by a meta-analysis review of 11 clinical trials with healthy volunteers showing that they directly and independently cause weight gain and insulin resistance [6]. Moreover, another meta-analysis evaluating both FGAs and SGAs efficacy and tolerability found that olanzapine (OLA), zotepine and clozapine, were the SGAs associated with higher weight gain [7]. These alterations from the beginning of the treatments may lead to complications such as T2D and cardiovascular disorders that might decrease patients' compliance and increase health costs [8].

Hyperphagia is believed to be the main cause of weight gain induced by short-term treatment with SGAs [9,10]. However, upon long-term administration, when food intake is normalized, reduction in energy expenditure (EE) due to defective brown adipose tissue (BAT) thermogenesis seems to be responsible for body weight gain [11]. BAT is abundant in mitochondria that are enriched in uncoupling protein-1 (UCP-1) in the inner membrane, which allows dissipation of chemical energy in the form of heat by uncoupling fuel oxidation from ATP synthesis [12]. Thermogenic function is considered an important regulator of whole-body energetic balance, since defects in this process result in weight gain and obesity in several mouse models [9,13]. In humans, BAT has been identified in several locations, mainly in the lower neck area, where its functionality is currently under extensive study [14]. Moreover, the possibility to recruit beige cells with high thermogenic potential within white adipose tissue (WAT) depots has opened the field for new strategies to combat obesity and its associated comorbidities [15].

Protein tyrosine phosphatase-1B (PTP1B) is a critical negative modulator of leptin and insulin signaling and a therapeutic target for obesity and T2D. This has been evidenced in preclinical studies in mice deficient in the *Ptpn1* gene (encoding PTP1B) that were protected against obesity [16–18]. Importantly, alterations in leptin levels have been reported in humans and rodents after acute or chronic treatment with OLA [19–21]. In this line, herein we hypothesize a potential beneficial effect of PTP1B inhibition in the context of OLA-induced weight gain. To address this issue, energy balance modulated by an inter-organ crosstalk between the hypothalamus and BAT/subcutaneous WAT (iWAT) was analyzed in WT and PTP1B-KO male mice receiving treatment with OLA either orally or intraperitoneally (i.p.), the main administration routes reported in previous studies [5,9].

2. Material and methods

Antibodies for Western blot and immunohistochemistry/immunofluorescence and primers used for qRT-PCR are listed in Supplementary Tables 1, 2 and 3 respectively. Additional details regarding methods can be found in Supplementary information.

2.1. Animals and treatments

Three-months-old wild-type (WT) and PTP1B-KO male mice on the C57BL/6 J x 129Sv/J genetic background [22] and age-matched C57BL/6 J male mice were used. Animal studies were approved by the Ethics Committee of CSIC and conducted in accordance with the guidelines for animal care of Comunidad de Madrid and Directive 2010/63/EU. Animals were maintained at 22–24 °C and 55 % humidity on 12 h light/dark cycles (starting at 8 am) and fed a regular rodent chow diet (A04, Panlab, Barcelona, Spain) and tap water ad libitum.

2.1.1. OLA-supplemented diet treatment

WT and PTP1B-KO mice were fed the same chow diet supplemented with OLA (GP8311, Glentham Life Sciences, Corsham, UK) for 7 months. OLA dosage in the diet was calculated taking into account an average mice weight of 30–35 g and food intake of 4 g/day, corresponding to 5 mg/kg/day. This dose was chosen based on previous studies in rodents treated orally with 5–10 mg/kg/day OLA showing hyperphagia and weight gain [10,23–25]. Body weight was monitored monthly and food intake was measured at month 5 of the treatment.

2.1.2. OLA intraperitoneal (i.p.) treatment

Mice received vehicle (VEH) (2 % *v*/v DMSO in 0.9 % NaCl) or 10 mg/kg/day OLA via i.p. injection (10–12 am) for 8 weeks as reported for injectable treatments [26–30]. Another cohort of mice was treated with OLA at 5 mg/kg/day. Body weight was monitored weekly. Food intake was measured manually at week 5 of treatment. OLA levels in plasma and hypothalamus were measured in mice receiving a single i.p. injection (5 or 10 mg/kg), after which they were sacrificed at 2, 4, 8 and 24 h.

2.1.3. OLA treatment by oral gavage

Mice received a daily (10–12 am) oral gavage of OLA at 10 mg/kg, dose previously reported for oral treatment [24,25,31–34] or vehicle (4 % *v*/v DMSO in 0.9 % NaCl) for 8 weeks. The animals were monitored for body weight and food intake. For the analysis of OLA levels in plasma and hypothalamus, mice received a single oral gavage of OLA (10 mg/kg) and sacrificed at 2, 4, 8 and 24 h.

2.1.4. OLA intrahypothalamic injections

During the light phase of the diurnal cycle (8 am-1 pm), mice were anesthetized with isoflurane for ~5 min prior to the intrahypothalamic injection and placed in the stereotaxic apparatus. Then, mice received bilaterally a single injection of OLA (15 nmol, dose used in a previous study [35]) or DMSO in the ventromedial nucleus of the hypothalamus (VMH) at the coordinates 1.46 mm posterior, ± 0.5 mm lateral and 5.5 mm depth to Bregma [36]. During the injection, mice remained anesthetized with isoflurane. To minimize backflow up the needle track, the needle remained inserted for approximately 3–5 min after injection. In another experiments, C57BL/6 J male mice were injected adenoviral vectors encoding for AMPKα1-CA and GFP (Viraquest, North Liberty, IA, USA) in the VMH using the same coordinates (1 µl/injection site) as previously reported [37–39], prior to the OLA central injection.

2.2. Brown adipocyte differentiation

Brown preadipocytes from lactating mice were immortalized and fully differentiated to mature brown adipocytes as previously described [40] and detailed in the Supplementary material.

2.3. GT1-7 culture

GT1-7 transformed hypothalamic neurosecretory cell line was kindly provided by Prof. P. Mellon (University of California San Diego, CA, USA) [41]. Cells were grown in DMEM supplemented with 10 % FBS, 2 mM glutamine (25030-024, Gibco, Waltham, MA, USA), 20 mM HEPES and antibiotics (100 U/ml penicillin, 100 µg/ml streptomycin (15140-

122, Gibco)). For experiments, cells were seeded at 7.5×10^4 cells/ml in 6-well plates and grown until confluence. Cells were then treated with OLA (12.5 μM) for different time periods ranging from 5 min to 24 h in serum-free medium.

2.4. Preparation of iWAT explants from mice and humans

iWAT pads from untreated mice were collected under sterile conditions and placed in a 6-well plate with pre-warmed (37 °C) serum-free DMEM supplemented with 0.2 % (*w/v*) BSA, 2 mM glutamine, 100 U/ml penicillin and 100 μg/ml streptomycin. Connective tissue and blood vessels were removed by dissection before finely mince the tissue. Explants were cultured with or without OLA at 0.2, 2 and 12.5 μM for 48 h. As a positive control of the browning capacity of the tissue, explants were treated overnight with a β3-adrenergic agonist (CL, CL326,243, Sigma-Aldrich) at 2 μM concentration.

Abdominal subcutaneous WAT biopsies were collected from 8 healthy individuals (6 women and 2 men; age: 21–74 years old; BMI: 22.9–35.0 kg/m^2), treated with OLA ex vivo and processed as described in [42].

2.5. Data analysis

Statistical analysis was performed with GraphPad Prism version-7.0 (GraphPad, Inc., San Diego, CA, USA). Data are reported as mean and standard error of the mean (SEM). Comparisons between groups were made using Student's *t*-test if 2 groups were considered. If >2 groups were studied with one variable taken into consideration (*i.e* treatment or genotype) One Way-ANOVA (α = 0.05) was used, with Bonferroni's test carried for multiple comparisons between the groups. When more than one variable was compared (*i.e* treatment and genotype) data were analyzed with Two Way-ANOVA (α = 0.05) with multiple comparisons by Bonferroni's post-hoc test. To ensure that changes in EE were independent of the weight of the mice, EE (Kcal/h) was also analyzed via ANCOVA [43] as reported [44]. If not indicated in the figure legend, Two Way-ANOVA with Bonferroni's post-hoc test was used for the statistical analysis.

3. Results

3.1. Differential effects of OLA i.p. and dietary treatment in body weight and EE in WT and PTP1B-KO male mice

We first evaluated food intake and body weight progression in WT and PTP1B-KO male mice fed a regular or OLA-supplemented diet (5 mg/kg/day) for 7 months. As shown in Fig. 1A, dietary administration of OLA increased food intake in both genotypes of mice. Therefore, considering OLA-induced hyperphagia, mice on dietary treatment received approximately 8–10 mg/kg/day. Taking this into account, another cohort of mice from both genotypes received daily i.p. injections of OLA at 10 mg/kg or VEH for 8 weeks and no alterations in food intake were found (Fig. 1B). WT mice fed an OLA-supplemented diet presented higher body weight gain than their controls, whereas mice lacking PTP1B were protected against weight gain (Fig. 1C, Supplementary Fig. 1A). Unexpectedly, male mice from both genotypes treated with OLA via i.p. showed a significant body weight loss (Fig. 1D, Supplementary Fig. 1B).

Body weight loss in OLA-treated male mice via i.p. was associated with a marked increase in whole-body EE, a mass-independent effect according to ANCOVA regression analysis (Fig. 1E, F), without changes in spontaneous locomotor activity (Fig. 1G), pointing the modulation of EE as a possible mechanism by which OLA administration via i.p. reduces body weight. Regarding the respiratory exchange rate (RER) (Supplementary Fig. 1C), only a slight, but significant, increase during the dark phase was found in OLA-treated PTP1B-deficient mice, suggesting a higher use of carbohydrates for energy production. On the

other hand, WT mice fed an OLA-supplemented diet presented reduced EE in both light and dark phases; being this effect also mass-independent (Fig. 1H, I), and less movement during the dark phase compared to their controls (Fig. 1J). Additionally, in WT mice RER was not affected by OLA (Supplementary Fig. 1D), suggesting that reduction of locomotor activity is not secondary to sedation. By contrast, PTP1B-KO mice did not show changes in locomotor activity, but presented a trend to elevated EE, reinforcing the relevance of EE in body weight control upon OLA treatment (Fig. 1H-J).

To substantiate the differential effects on body weight depending on the administration route, another cohort of mice was treated with OLA (10 mg/kg/day) by oral gavage for 8 weeks. As observed in the dietary treatment, OLA did not reduce body weight when administered via oral gavage (Supplementary Fig. 1E). Notably, in the first 2 weeks of treatment, neither i.p. nor oral gavage administration resulted in changes in food intake (Supplementary Fig. 1F). Nevertheless, and opposite to the observations in the i.p. treatment, administration of OLA by oral gavage increased cumulative food intake after 7 weeks (Supplementary Fig. 1G). Altogether, these results led us to propose that the i.p. treatment might be beneficial in preventing body weight gain associated with OLA and even predispose mice to lose weight.

3.2. Differential effects of OLA i.p. and dietary treatment in BAT thermogenesis in WT and PTP1B-KO male mice

Since mice treated with OLA via i.p., independently of the genotype, presented body weight loss and increased EE, we analyzed BAT thermogenesis. Increased UCP-1 protein levels were detected in BAT from WT and PTP1B-KO OLA-treated mice (Fig. 2A). This was associated with elevated BAT temperature in both genotypes, although this effect was significant only in WT mice probably due to the higher basal BAT temperature of PTP1B-KO mice (Fig. 2B). Tail temperature was also elevated in PTP1B-KO mice receiving OLA via i.p. (Fig. 2B), an effect that has been associated with heat dissipation and whole-body thermoregulation [45]. Moreover, type 2 deiodinase (DIO2), a positive UCP-1 modulator, was increased in BAT from WT and PTP1B-KO mice receiving i.p. treatment with OLA (Fig. 2C). However, no differences were found in Tyrosine Hydroxylase (TH) protein levels. BAT sections from those mice evidenced activation features manifested by reduced lipid droplet size (Fig. 2D, Supplementary Fig. 2A, B) in parallel with increased UCP-1 immunostaining (Fig. 2D).

On the other hand, in WT mice fed an OLA-supplemented diet, BAT UCP-1 levels were comparable to those of the control group, while PTP1B-KO mice showed a marked increase in line with enhanced EE (Figs. 2E, 1G). Also, BAT temperature showed a tendency to increase in PTP1B-KO animals treated orally with OLA, together with a significant increase in tail temperature (Fig. 2F). Importantly, EE (Supplementary Fig. 3A), BAT and tail temperature (Supplementary Fig. 3B and C) and BAT UCP-1 protein levels (Supplementary Fig. 3D) were unchanged in mice receiving OLA by oral gavage. Overall, these results suggest that changes in body weight are associated with EE and BAT thermogenesis in OLA-treated mice.

3.3. Hypothalamic AMPK phosphorylation controls BAT thermogenesis in mice treated with OLA via i.p.

Of interest, the elevation of UCP-1 protein levels was not observed in differentiated brown adipocytes treated in vitro with OLA at concentrations that preserved cell viability (Supplementary Fig. 4A, B), pointing to an inter-organ crosstalk in the modulation of body weight and EE by OLA in mice.

Based on the previously reported relevance of hypothalamic AMPK in controlling BAT thermogenesis in the context of the central effects of thyroid hormones [37,39], we determined AMPK phosphorylation in the hypothalamus of mice receiving OLA i.p. treatment that presented a marked increase in BAT UCP-1 levels in both genotypes (Fig. 2A).
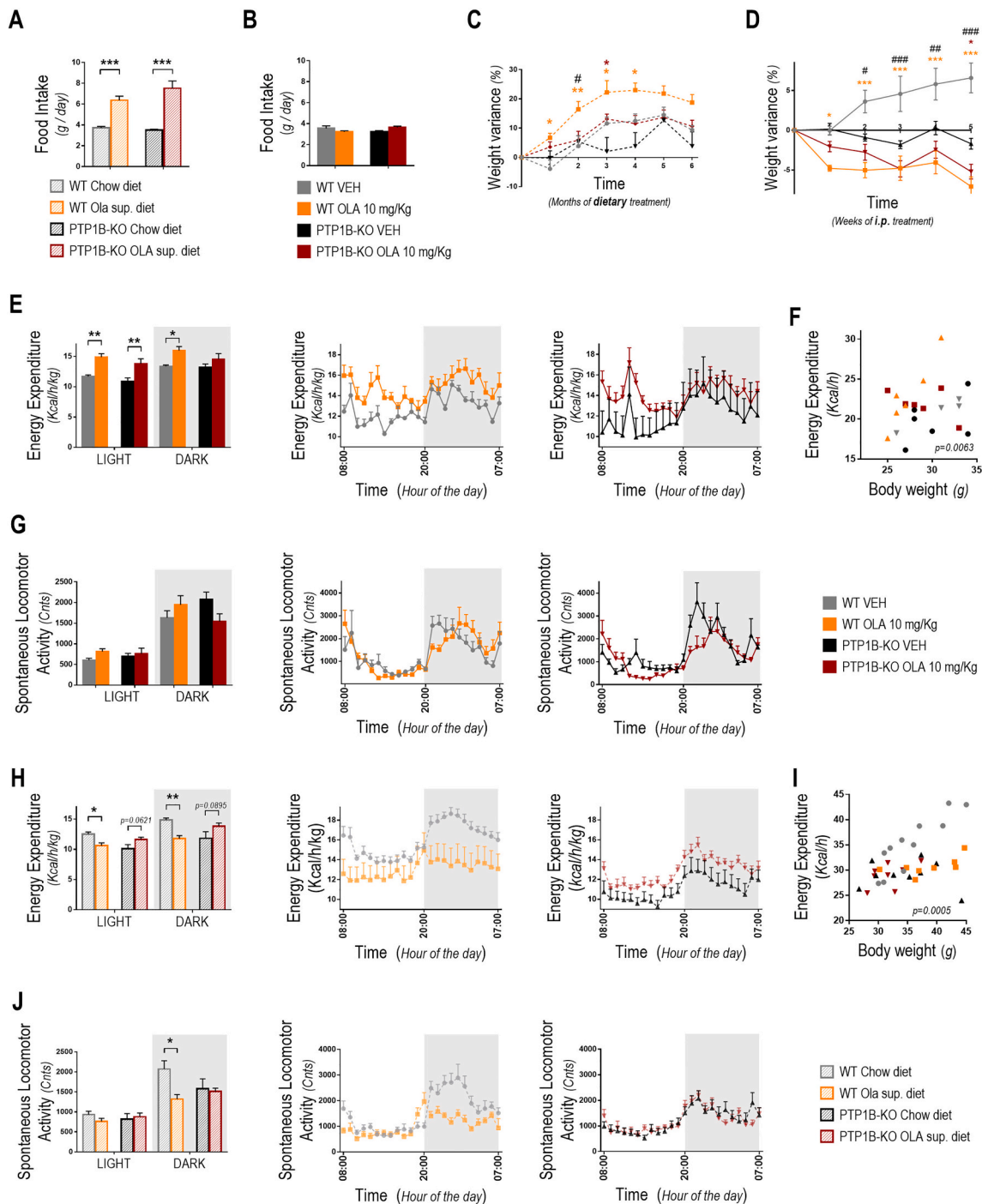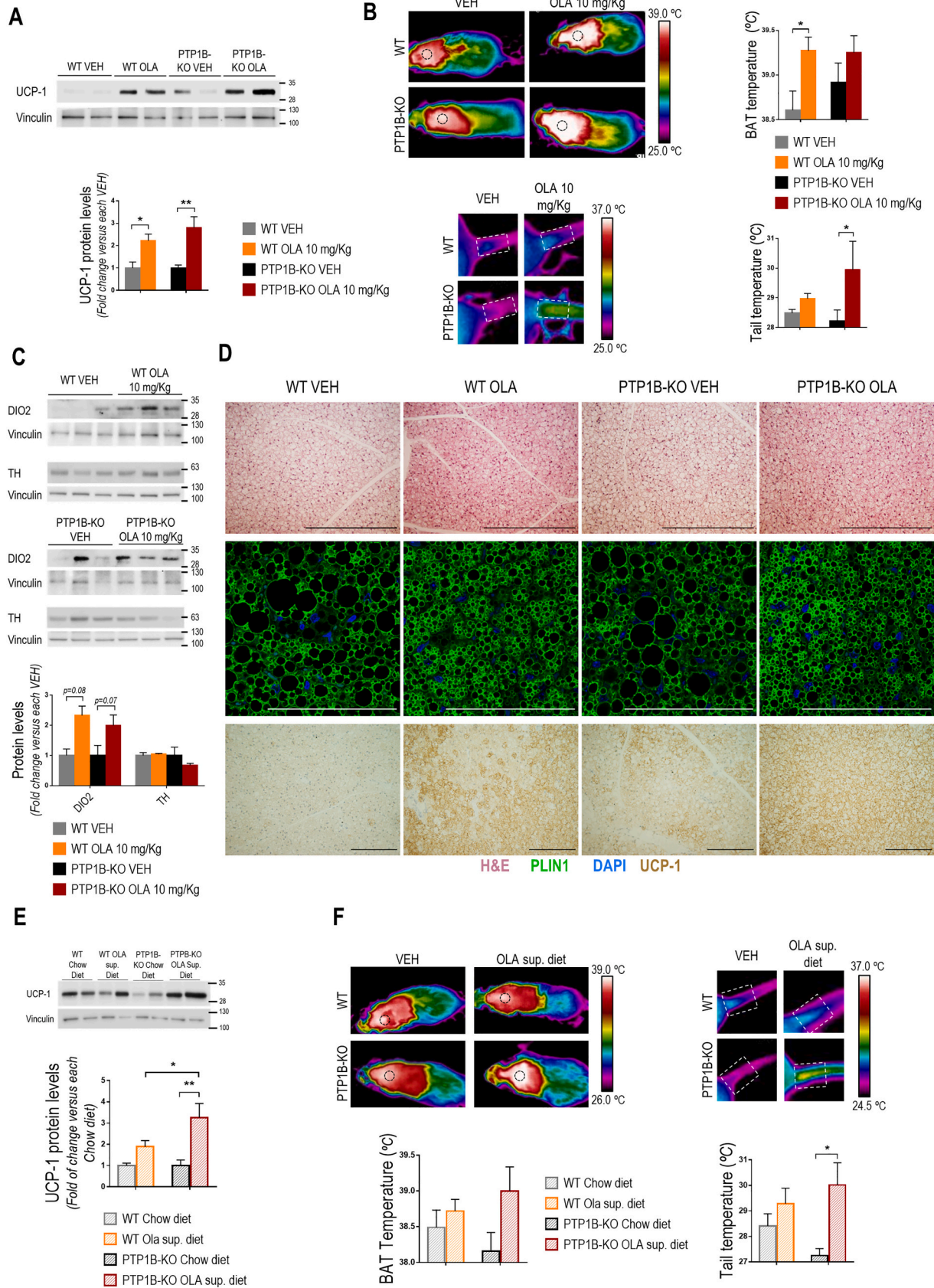
Fig. 1. Differential effects of OLA i.p. and dietary treatment in body weight and energy expenditure in WT and PTP1B-KO male mice. WT and PTP1B-KO male mice received a daily i.p. injection of OLA (10 mg/kg) during 8 weeks or OLA-supplemented diet (5 mg/kg) for 7 months. A. Daily food intake for one week at month 5 of OLA dietary treatment (WT Chow diet: $n = 32$; WT OLA sup. diet: $n = 21$; PTP1B-KO Chow diet: $n = 33$; PTP1B-KO OLA sup. diet: $n = 19$). B. Daily Food intake measured manually for one week at week 5 of OLA i.p. treatment (WT VEH: n = 21; WT OLA: n = 21; PTP1B-KO VEH: $n = 20$; PTP1B-KO OLA: $n = 23$). C. Monthly body weight variance in mice receiving OLA-supplemented diet (WT Chow diet: $n = 10$; WT OLA sup. diet: n = 10; PTP1B-KO Chow diet: $n = 9$; PTP1B-KO OLA sup. diet: $n = 10$). D. Weekly body weight variance throughout OLA i.p. treatment (WT VEH: $n = 6$; WT OLA: $n = 6$; PTP1B-KO VEH: n = 9; PTP1B-KO OLA: $n = 11$) E. Energy expenditure (EE) of the experimental groups under i.p. treatment measured by indirect calorimetry (WT VEH: $n = 4$; WT OLA: $n = 6$; PTP1B-KO VEH: n = 6; PTP1B-KO OLA: $n = 6$). F. ANCOVA regression analysis of the EE of the groups treated via i.p. injection versus body weight (WT VEH: $n = 4$; WT OLA: $n = 6$; PTP1B-KO VEH: n = 6; PTP1B-KO OLA: $n = 6$). G. Spontaneous locomotor activity of the experimental groups under i.p. treatment (WT VEH: $n = 4$; WT OLA: $n = 6$; PTP1B-KO VEH: n = 6; PTP1B-KO OLA: $n = 6$). H. EE of the experimental groups receiving OLA-supplemented diet (WT Chow diet: $n = 11$; WT OLA sup. diet: $n = 8$; PTP1B-KO Chow diet: $n = 9$; PTP1B-KO OLA sup. diet: $n = 8$). I. ANCOVA regression analysis of the EE of the groups receiving OLA-supplemented diet versus body weight (WT Chow diet: n = 11; WT OLA sup. diet: n = 8; PTP1B-KO Chow diet: n = 9; PTP1B-KO OLA sup. diet: n = 8). J. Spontaneous locomotor activity of the experimental groups receiving OLA-supplemented d diet (WT Chow diet: $n = 13$; WT OLA sup. diet: n = 8; PTP1B-KO Chow diet: n = 11; PTP1B-KO OLA sup. diet: n = 8). Each point/bar corresponds to mean ± SEM; Each point/bar corresponds to mean ± SEM; comparisons between groups: * $p < 0.05$; ** $p < 0.01$; *** $p < 0.001$.

A

B

C

D

H&E   PLIN1   DAPI   UCP-1

E

F

(caption on next page)

Fig. 2. Differential effects of OLA i.p. and dietary treatment in BAT thermogenesis in WT and PTP1B-KO male mice. A. Representative Western blot of BAT UCP-1 and densitometric quantification normalized for Vinculin levels in mice treated with OLA via i.p. (WT VEH: $n = 5$; WT OLA: n = 5; PTP1B-KO VEH: $n = 6$; PTP1B-KO OLA: n = 6). B. Thermographic pictures and quantification of BAT *(upper panel)* and tail *(lower panel)* maximal temperature of VEH- and OLA- treated male mice via i.p. (WT VEH: $n = 10$; WT OLA: $n = 17$; PTP1B-KO VEH: $n = 7$; PTP1B-KO OLA: n = 7). C. Representative Western blots of DIO2 and TH in BAT of WT *(upper panel)* and PTP1B-KO *(middle panel)* mice treated with OLA via i.p. Densitometric quantification normalized for Vinculin levels *(lower panel)* (WT VEH: $n = 3$; WT OLA: n = 4; PTP1B-KO VEH: n = 5; PTP1B-KO OLA: $n = 6$). D. Representative H&E images of BAT (20×, scale bars-100 μm, *upper images*), PLIN1 immunofluorescence analyzed by confocal microscopy (63×, scale bars-100 μm, *middle images*) and UCP-1 immunohistochemistry (20×, scale bars-100 μm, *lower images*) of mice treated with OLA via i.p. (WT VEH: $n = 3$; WT OLA: n = 3; PTP1B-KO VEH: n = 3; PTP1B-KO OLA: n = 3). E. Representative Western blot of BAT UCP-1 and densitometric quantification normalized for Vinculin levels in mice receiving OLA supplemented in the diet (WT Chow diet: n = 6; WT OLA sup. diet: $n = 9$; PTP1B-KO Chow diet: n = 6; PTP1B-KO OLA sup. diet: n = 7). F. Thermographic pictures *(upper panel)* and quantification of BAT and tail *(lower panel)* maximal temperature in mice receiving OLA supplemented in the diet (BAT: WT Chow diet: $n = 19$; WT OLA sup. diet: $n = 10$; PTP1B-KO Chow diet: $n = 9$; PTP1B-KO OLA sup. diet: $n = 8$; Tail: WT Chow diet: n = 19; WT OLA sup. diet: n = 10; PTP1B-KO Chow diet: n = 9; PTP1B-KO OLA sup. diet: n = 6). Each point/bar corresponds to mean ± SEM; comparisons between groups: * $p < 0.05$; ** $p < 0.01$; *** $p < 0.001$.

Fig. 3A shows diminished hypothalamic phospho-AMPK in WT and PTP1B-KO mice upon OLA i.p. administration. Notably, this effect was absent in the hypothalamus of mice fed an OLA-supplemented diet (Fig. 3B) or mice treated by oral gavage (Supplementary Fig. 4C). To substantiate these results, we tested the direct effect of OLA in the hypothalamic neuron cell line GT1-7 and a reduction of phospho-AMPK was found (Fig. 3C) without compromising cell viability (Supplementary Fig. 4D).

To further investigate the direct effect of OLA in modulating AMPK phosphorylation in the hypothalamus and, hence, BAT UCP-1 levels, WT mice received an intrahypothalamic injection of OLA and the hypothalami were collected after 30 min or 8 h. As shown in Fig. 3D and Supplementary Fig. 4E, hypothalamic phospho-AMPK was reduced in parallel to an increase in BAT UCP-1 levels in the absence of TH modulation. Notably, no changes in food intake were found up to 48 h post-intrahypothalamic OLA injection (Supplementary Fig. 4F). In another cohort of mice, a constitutively active version of AMPKα1 (AMPKα1-CA) was overexpressed in the hypothalamus by adenoviral central injection 5 days prior to OLA intrahypothalamic administration [37,39,46]. As shown in Fig. 3E, GFP signal was visualized 5 days after adenoviral delivery. Importantly, AMPKα1-CA prevented OLA-induced increase in BAT UCP-1 protein levels. These data support the relevance of AMPK activation status in the hypothalamic control of UCP-1 levels in BAT in response to OLA.

Next, we interrogated whether the different effects of the i.p. and oral treatment in AMPK-driven hypothalamic-BAT axis were related to OLA levels reaching the hypothalamus. To achieve this, we measured hypothalamic OLA levels upon a single dose (10 mg/kg) administered via i.p. or oral gavage by liquid chromatography-tandem mass spectrometry (LC-MS/MS) in extracts from this brain region, as detailed in the Supplementary material. As shown in Fig. 3F, hypothalamic OLA levels peaked at 2 h; being almost 2.5-fold higher when OLA was administered via i.p. These results suggest that the levels of OLA required to modulate hypothalamic AMPK are likely not achieved in the oral treatment. As expected, OLA levels in plasma paralleled those reached in the hypothalamus (Fig. 3F). Moreover, mRNA levels of *Cyp1a2*, encoding the main enzyme that metabolizes OLA in the liver [47], remained unchanged (Supplementary Fig. 5A). To ensure that the modulation of AMPK phosphorylation relays in hypothalamic OLA levels, mice were treated with OLA via i.p. injection at 5 mg/kg/day. Of note, under this lower dose, the peaks of OLA levels in plasma and hypothalamus were ~2.5-fold lower than those of the 10 mg/kg i.p. injection and, importantly, both peaks were similar to those reached by the oral gavage (Supplementary Fig. 5B). Moreover, mice receiving the chronic treatment with OLA via i.p. at 5 mg/kg/day did not show reductions in body weight or hypothalamic phospho-AMPK and also did not present increased BAT UCP-1 levels (Supplementary Fig. 5C-E). These results support that the levels of OLA reaching the hypothalamus might be crucial for decreasing AMPK phosphorylation in this brain region which activates BAT thermogenesis.

3.4. Activation of iWAT browning by increased sympathetic innervation and decreased sympathetic neuron-associated macrophages (SAMs) upon OLA treatment via i.p. in male mice

In addition to BAT, browning of iWAT contributes to whole-body energy balance [48]. The analysis of iWAT revealed an up-regulation of UCP-1 protein levels in WT and PTP1B-KO mice receiving OLA treatment via i.p. that paralleled with an increase in TH levels (Fig. 4A), suggesting enhanced sympathetic innervation in this fat depot. This was confirmed by the analysis of TH positive nervous fibers (Fig. 4B). Additionally, changes in iWAT morphology manifested by reduced lipid droplet size were induced by OLA in either WT or PTP1B-KO mice (Fig. 4B, Supplementary Fig. 4A), thereby reflecting thermogenic activation of this fat depot. Moreover, double TH-F4/80 immunostaining of iWAT tissue (Fig. 4C, Supplementary Videos 1–4) revealed reduced presence of SAMs in mice from both genotypes receiving OLA via i.p. Again, iWAT browning was not found in mice fed an OLA-supplemented diet (Fig. 4D). These results highlight the synergism between central and intra-tissue signals in the activation and browning of iWAT by OLA.

To understand whether OLA directly induces browning, iWAT explants from WT mice were treated with different concentrations of OLA (Fig. 5A). As a positive control, iWAT explants from WT mice were treated with the β3-adrenergic agonist CL316,243 (2 μM) and, as expected, UCP-1 and TH levels were increased (Fig. 5A). However, UCP-1 levels did not increase by OLA. Similar results were found in human explants of subcutaneous fat (Fig. 5B). Since it has been previously reported that hypothalamic AMPK also modulates WAT browning [49], we investigated a possible role of the hypothalamus in OLA-mediated effects in iWAT. For this goal, WT mice received OLA via intrahypothalamic injection and, as shown in Fig. 5C, elevations in UCP-1 and TH were observed at 48 h post-injection. A step further, in another cohort of mice AMPKα1-CA was overexpressed in the hypothalamus by adenoviral central injection as described above (Fig. 5D) [37,39]. Importantly, AMPKα1-CA prevented OLA-induced elevation of iWAT UCP-1 protein levels (Fig. 5D). These data support the relevance of AMPK activation status in the hypothalamic control of iWAT browning in response to OLA.

4. Discussion

Preclinical studies have been conducted to unravel the metabolic side-effects associated with SGAs [5,9]; being OLA the focus of many of them due to body weight gain and insulin resistance found in patients under treatment [50]. Herein, we report unexpected differences in body weight by administering OLA orally by diet supplementation/oral gavage or via i.p. injections. Both routes have been used in studies in rodents at similar doses [10,23–34,51]. At the molecular level, we found firstly that PTP1B inhibition prevented weight gain in male mice during long-term oral treatment with OLA. Secondly, we unraveled PTP1B-independent effects of OLA i.p. administration in BAT activation and iWAT browning through a central-peripheral inter-organ crosstalk governed by hypothalamic AMPK and leading to weight loss.
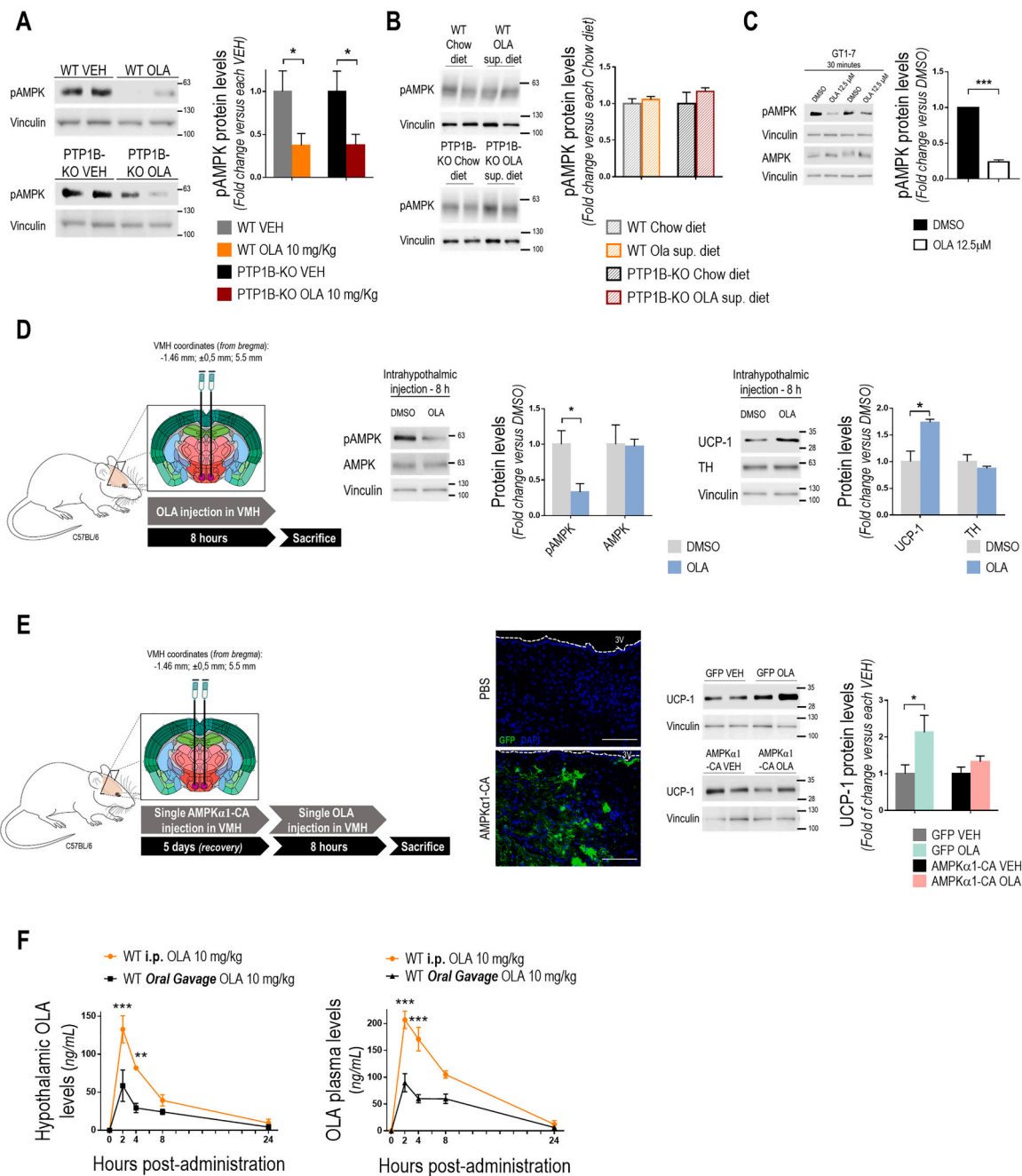
Fig. 3. Hypothalamic phosphorylation status of AMPK controls BAT thermogenesis in male mice treated with OLA via i.p. A. Representative Western blots of hypothalamic AMPK phosphorylation in OLA-treated mice via i.p. and densitometric quantification normalized for Vinculin levels (WT VEH: n = 8; WT OLA: n = 9; PTP1B-KO VEH: n = 8; PTP1B-KO OLA: $n = 13$). B. Representative Western blots of AMPK phosphorylation in the hypothalamus of WT and PTP1B-KO mice receiving OLA-supplemented diet for 7 months (WT Chow diet: $n = 6$; WT OLA sup. diet: n = 6; PTP1B-KO Chow diet: $n = 4$; PTP1B-KO OLA sup diet: n = 6). C. Representative Western blot of AMPK phosphorylation in GT1–7 hypothalamic neurons treated with OLA (12.5 μM) for 30 min and densitometric quantification normalized for Vinculin levels (DMSO: $n = 3$; OLA 12.5 μM: n = 3, groups were compared using Student's *t*-test). D. Experimental design (*left panel*). Representative Western blots of hypothalamic AMPK phosphorylation and total AMPK in WT male mice 8 h after receiving an intrahypothalamic injection with OLA (15 nmol) (*middle panel*) and densitometric quantification normalized for Vinculin levels (WT VEH: n = 3; WT OLA: n = 3, groups were compared using Student's t-test). Representative Western blot of BAT UCP-1 in WT male mice under conditions described in D with respective densitometric quantification normalized for Vinculin levels (*right panel*) (WT VEH: n = 3; WT OLA: n = 3, groups were compared using Student's t-test). E. Experimental design of the adenoviral intrahypothalamic injection of constitutively activated AMPKα1 in male mice 5 days prior to a single OLA (15 nmol) intrahypothalamic injection and BAT collection after 8 h (*left panel*). Representative confocal microscopy GFP immunofluorescence (25×, scale bars-100 μm) showing exogenous AMPK (*middle panel*). Representative Western blot of BAT UCP-1 in male mice injected AMPKα1-CA or GFP adenoviruses 5 days prior to OLA or DMSO intrahypothalamic injection and respective densitometric quantification normalized for Vinculin levels (*right panel*) (GFP VEH: $n = 7$; GFP OLA: $n = 6$; AMPKα1-CA VEH: $n = 6$; AMPKα1-CA OLA: n = 7). F. OLA levels in extracts from hypothalamus of WT male mice treated with a single dose of OLA via i.p. injection or receiving a single oral gavage (i.p.: 2 h $n = 4$; 4 h n = 4; 8 h n = 4; 24 h $n = 3$; oral gavage: 2 h n = 4; 4 h n = 4; 8 h n = 3; 24 h n = 4). OLA plasma levels in WT male mice treated with a single dose of OLA via i.p. injection or receiving a single oral gavage (i.p.: 2 h n = 5; 4 h n = 5; 8 h n = 4; 24 h n = 4; oral gavage: 2 h n = 4; 4 h n = 4; 8 h n = 3; 24 h n = 3). Each point/bar corresponds to mean ± SEM; comparisons between groups: * $p < 0.05$; ** $p < 0.01$; *** $p < 0.001$.
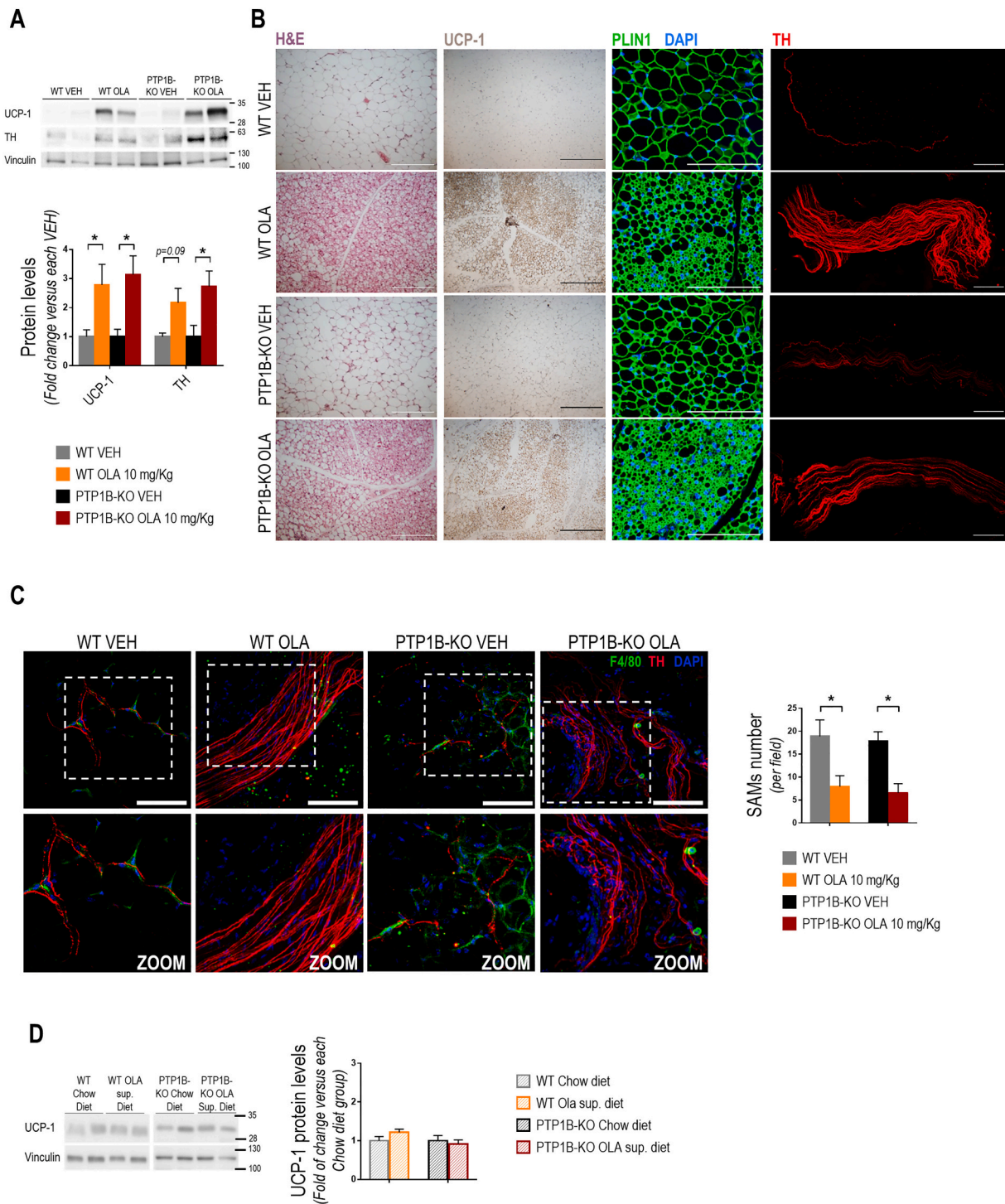
Fig. 4. Activation of iWAT browning through increased sympathetic innervation and decreased sympathetic neuron-associated macrophages (SAMs) in male mice treated with OLA via i.p. A. Representative Western blots of UCP-1 and TH in iWAT and densitometric quantification normalized for Vinculin levels in WT and PTP1B-KO mice receiving OLA via i.p. (WT VEH: $n = 12$; WT OLA: $n = 14$; PTP1B-KO VEH: $n = 11$; PTP1B-KO OLA: $n = 11$). B. Representative H&E images of iWAT ($20\times$, scale bars-100 μm, *left images*); UCP-1 immunohistochemistry ($20\times$, scale bars-100 μm, *middle left images*); PLIN1 immunofluorescence ($20\times$, scale bars-50 μm, *middle right images*) (WT VEH: $n = 3$; WT OLA: n = 3; PTP1B-KO VEH: $n = 3$; PTP1B-KO OLA: $n = 3$) and immunofluorescence of TH positive fibers analyzed by confocal microscopy ($25\times$, scale bars-100 μm, *right images*) of OLA-treated mice via i.p. (WT VEH: $n = 5$; WT OLA: n = 5; PTP1B-KO VEH: $n = 4$; PTP1B-KO OLA: n = 4). C. Representative immunofluorescence of TH positive fibers and F4/80 positive cells in iWAT analyzed by confocal microscopy ($25\times$, scale bars-100 μm, *upper images*) and respective zoom (*lower panel*) and quantification (WT VEH: $n = 7$; WT OLA: n = 6; PTP1B-KO VEH: $n = 5$; PTP1B-KO OLA: n = 4). D. Representative Western blots of UCP-1 in iWAT and densitometric quantification normalized for Vinculin levels in mice receiving OLA supplemented diet (WT Chow diet: n = 6; WT OLA sup. diet: $n = 9$; PTP1B-KO Chow diet: n = 6; PTP1B-KO OLA sup diet: n = 7). Each point/bar corresponds to mean ± SEM; comparisons between groups: * $p <$ 0.05; ** $p < 0.01$; *** $p < 0.001$.
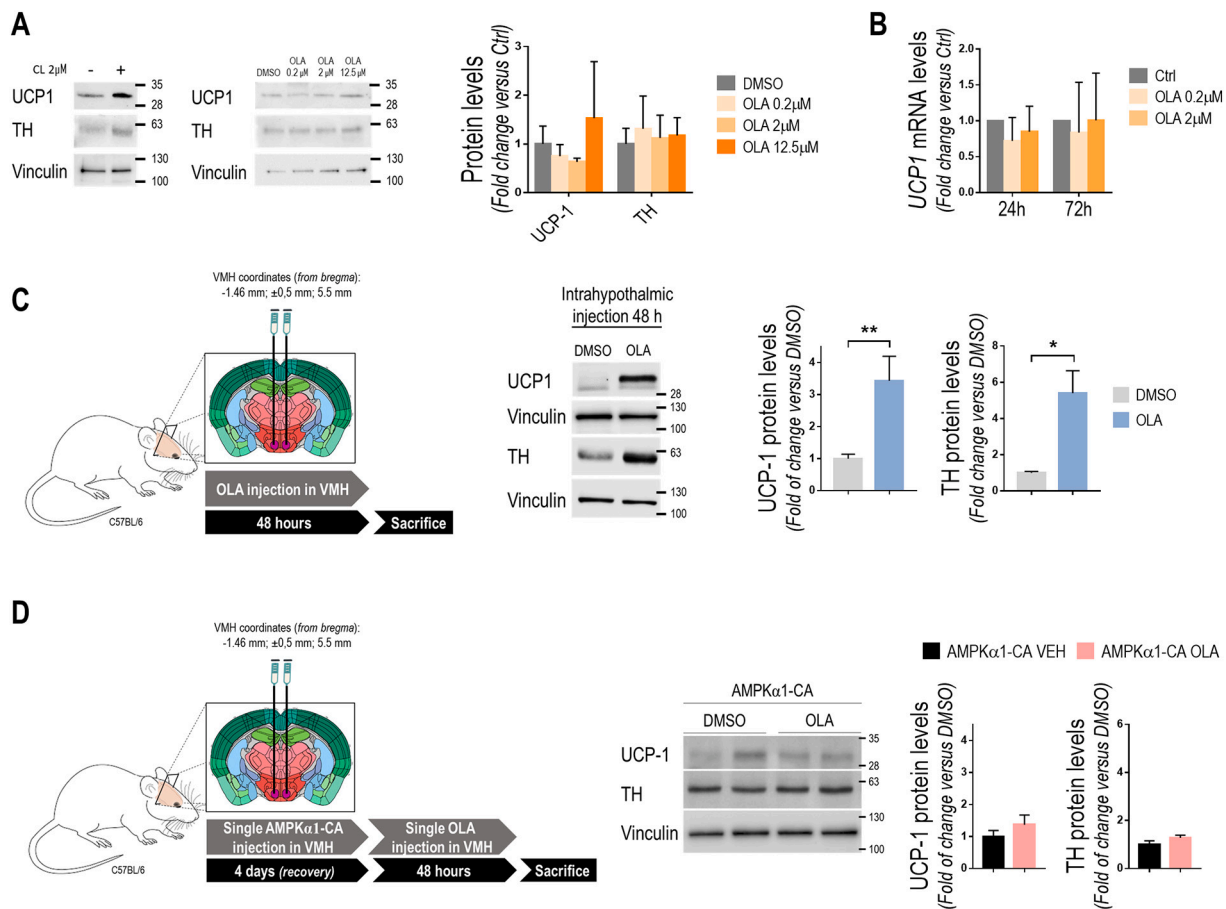
Fig. 5. Hypothalamic AMPK controls iWAT browning in i.p. OLA-treated mice. A. Representative UCP-1 and TH Western blots in iWAT explants stimulated with the β3-adrenergic agonist CL316,243 (2 μM) or treated with OLA (0.2, 2 and 12.5 μM) for 48 h and densitometric quantification normalized for Vinculin levels (n = 3 *per* condition). B. *UCP1* mRNA levels in human explants of subcutaneous adipose tissue stimulated with OLA (0.2 and 2 μM) for 24 and 72 h. *GAPDH* was used as housekeeping gene ($n = 8$ *per* condition). C. Experimental design *(left panel)*. Representative Western blots of UCP-1 (WT VEH: $n = 13$; WT OLA: $n = 16$; groups were compared using Student's *t*-test) and TH (WT VEH: n = 5; WT OLA: n = 6; groups were compared using Student's t-test) in iWAT from WT male mice 48 h after an intrahypothalamic OLA injection normalized for Vinculin levels *(right panel)*. D. Experimental design of the adenoviral intrahypothalamic injection of constitutively active AMPKα1 in male mice 4 days prior to OLA (15 nmol) intrahypothalamic injection and iWAT collection at 48 h. Representative BAT UCP-1 Western blot of and densitometric quantification normalized for Vinculin levels (AMPKα1-CA VEH: $n = 10$; AMPKα1-CA OLA: n = 10). Each point/bar corresponds to mean ± SEM; comparisons between groups: * $p < 0.05$; ** $p < 0.01$; *** $p < 0.001$.

To understand the molecular basis behind the weight loss induced by OLA i.p. administration and considering previous studies that point signals emerging from the hypothalamus as key modulators of systemic energy balance and weight control [39,52–56], we focused our research in the hypothalamic AMPK-BAT axis [57]. It has been demonstrated that a reduction of hypothalamic phospho-AMPK by T_3, estradiol, bone morphogenetic protein 8b (BMP8b) or nicotine led to an increase in BAT UCP-1 [37–39,49]. Therefore, this hypothalamic AMPK-BAT UCP-1 axis could also explain the effect of OLA administered via i.p. in male mice. Of interest, this molecular signature was associated with an increase in DIO2 protein levels, a well-known UCP-1 positive modulator [58], but not TH. In addition, BAT activation by OLA injections was histologically evidenced by smaller lipid droplets. Of relevance, OLA failed to increase UCP-1 in differentiated brown adipocytes. This evidence, together with the elevation of BAT UCP-1 concomitant with a reduction of hypothalamic phospho-AMPK in mice receiving an OLA intrahypothalamic injection, strongly supports the hypothalamus-BAT crosstalk as responsible for the increased BAT temperature and EE during the OLA i. p. treatment in male mice, leading to weight loss.

Of relevance, OLA downregulated phospho-AMPK in GT1–7 hypothalamic neurons, suggesting a direct effect in this cell population in triggering the central-peripheral interactome. Chen et al. reported an increase in phospho-AMPK in NPY-GFP hypothalamic neurons treated with OLA [59]. However, they used a higher concentration (25 μM) for longer time (3 h) compared to our experimental setting (12.5 μM for 30 min). Additionally, NPY neurons are mainly found in the arcuate nucleus (ARC) [60], while GT1–7 cells are gonadotropin-releasing hormone-expressing and -secreting neurons that are enriched in the VMH [61]. It is noteworthy to highlight that the VMH is the main hypothalamic region regulating whole body energy balance. In fact, we found that constitutive activation of AMPKα1, previously reported to control VMH-induced thermogenesis specifically in this hypothalamic region [38,39,49,62], prevented OLA-induced UCP-1 elevation in BAT, evidencing AMPK as a key controller of BAT thermogenesis in the OLA i. p. treatment. In this line, the work of Skrede et al. suggests a striking importance of OLA effects in the different hypothalamic nuclei [63]. In particular, a single intramuscular injection (70 mg/kg) in female rats after adenoviral inhibition of AMPK specifically in the ARC reduced hyperphagia and weight gain compared to the controls, as also supported by another study [64]. Interestingly, hyperphagia and weight gain upon OLA intramuscular injection at 100 mg/kg was not altered by AMPK inhibition in the VMH [63]. Of note, these results are not discordant with ours, since we found inhibition of OLA-induced UCP-1 in BAT upon constitutive AMPKα1 activation in the VMH. Importantly, hyperphagia was not found by OLA administration via i.p. neither at the beginning nor at week 5 of the treatment, suggesting the absence of OLA

orexigenic effects through activation of ARC signals under our experimental conditions. Thus, these studies support the specific control of feeding behavior by the ARC whereas the VMH is mainly responsible for controlling energy balance, as reviewed [62]. Furthermore, He et al. showed that hyperphagia was induced in female rats receiving OLA in cookie dough (3 mg/kg/day) at early stages of the treatment which correlated with increased phospho-AMPK in hypothalamic extracts and body weight gain [65]. Nonetheless, the work of Ferno et al. in female rats shows that hyperphagia induced by OLA oral administration is mediated through changes in hypothalamic neuropeptides in an AMPK-independent manner [64] in agreement with our results in male mice receiving OLA orally. Notably, our data show that a single OLA i.p. injection in the VMH negative modulates hypothalamic AMPK phosphorylation which, as mentioned above, activates BAT thermogenesis. Importantly, the above-mentioned studies were conducted in female rodents and OLA orexigenic effects were lost when this SGA was administered to ovariectomized rats [66] indicating that estradiol could play a role in OLA-induced hyperphagia and strongly suggesting that these effects might be gender dependent. In this regard, OLA effects in female mice receiving treatment via i.p., as well as the potential impact of estrogens in the activation of hypothalamus-BAT/iWAT axis, are currently under investigation. Related with gender dimorphism, our results contrast with the study of Ferno et al. [67] in male rats in which intramuscular OLA injections did not activate BAT, but led to less weight gain compared to vehicle-treated rats. These discrepancies can be due to the treatment duration (16 days in the study of Ferno et al. versus 8 weeks in our study), and/or differences in drug metabolism between species or formulation since they used a long-acting version of OLA.

Another issue addressed herein for the first time is the relation between activation of the hypothalamic AMPK-BAT UCP-1 axis and OLA levels reaching the hypothalamus. Male mice under oral treatment show hyperphagia, even at long time-periods, which favors weight gain; this effect being correlated with lower hypothalamic OLA levels and absence of BAT activation. By contrast, this dose (10 mg/kg) administered via i.p. resulted in higher OLA levels in the hypothalamus and activated the hypothalamus-BAT crosstalk resulting in weight loss. The need to overcome a threshold of OLA levels for activating this molecular pathway was also supported by an i.p. treatment with a lower dose (5 mg/kg/day) which failed to induce weight loss. Notably, and related with feeding activating mechanisms, in male mice treated with OLA by either i.p. injection or oral gavage we did not observe the increase in food intake found in female rats [63–65] even in the early stage of the treatment, suggesting that the molecular mechanisms linked to hyperphagia might be delayed in male mice. Moreover, since hyperphagia was exclusively found in mice treated orally with OLA, it is tempting to assume that the lower dose reaching the hypothalamus under this experimental setting can activate, due to anatomical proximity [68,69], the feeding-related molecular mechanisms of the ARC. However, in the i.p. treatment at 10 mg/kg, a higher dose of OLA reaches the hypothalamus and, under these conditions, the ARC signals might be suppressed by activation of the VMH, as reported [70,71], arising VMH also as a central satiety center. Very recently, Sternson et al. found excitatory projections of the VMH neurons to anorexigenic POMC neurons, strongly supporting that VMH reduces food intake by activating POMC neurons in the ARC and not by inhibiting orexigenic NPY neurons [72]. Taking all these into consideration, we suggest that OLA administered by i.p. might be beneficial to avoid weight gain associated with the oral administration.

It is noteworthy to highlight that, in humans, metformin, a well-known AMPK activator, has been used as an adjuvant for ameliorating OLA-induced weight gain and metabolic dysfunction [73]. However, the central effects of metformin were not clearly associated with modulation of AMPK activity. Metformin blocked AMPK activation and inhibited NPY expression in rat hypothalamic neurons under low glucose conditions [74]. Moreover, when centrally administered to rodents, metformin prevented ghrelin-induced stimulation of NPY and AgRP via

blockade of AMPK activation [75], supporting its ability to reduce food intake by decreasing the orexigenic peptides in the hypothalamus. However, another in vivo study in rats receiving metformin via central administration showed anorexigenic effects in an AMPK-independent manner, an effect possibly related to STAT3-mediated signaling [76]. Thus, metformin might regulate the feeding behavior by modulation of several appetite regulatory pathways. Additionally, oral metformin administration increases BAT UCP-1 levels in obese mice, as we recently reported [77]. Overall, our results point that OLA administration via i.p. could be an alternative to replace metformin or other combinatorial treatments in order to avoid additional adverse side-effects.

Interestingly, our results reveal that PTP1B inhibition, which impacts on central and peripheral metabolic control [22,78–80], does not influence the hypothalamus-BAT axis in response to OLA i.p. administration. In agreement with previous data [81], BAT sections from PTP1B-KO mice contained more UCP-1 positive areas which likely contribute to their inherent protection against obesity. However, differences in basal UCP-1 levels were not observed in aged mice (control mice at the end of the dietary treatment). BAT temperature was also elevated in young PTP1B-KO mice under basal conditions when compared to age-matched WT animals, but both genotypes reached similar BAT temperature upon OLA i.p. treatment. The augmented basal BAT UCP-1 of global PTP1B-deficient mice seems not to be mediated by deletion of this phosphatase in the hypothalamus since Tsou et al. reported no differences in basal *Ucp1* expression in BAT from mice with hypothalamic PTP1B deficiency [82]. In fact, PTP1B re-expression in PTP1B-KO brown adipocytes reduces UCP-1 [83], reinforcing a direct effect of this phosphatase in BAT. It is also relevant to mention that PTP1B-KO mice presented higher tail temperature upon OLA administration, either oral or i.p., reflecting a better heat dissipation capacity through vasodilatation. On the other hand, PTP1B-KO mice under the OLA dietary treatment did not present abnormal weight gain. Although hyperphagia was comparable with that of WT mice, animals lacking PTP1B had higher EE, an effect likely due to BAT thermogenesis. Since we did not find a decrease in hypothalamic phospho-AMPK levels, BAT activation in those mice likely rely on mechanisms different to those in the i.p. treatment, for instance, exacerbated diet-induced thermogenesis. Future experiments will elucidate whether BAT activation in PTP1B-deficient mice is induced by OLA-mediated hyperphagia. So far, although clinical trials are being conducted with PTP1B inhibitors such as trodusquemine (i.e., NCT00606112), none of them are currently approved for clinical use. Interestingly, it has been reported that schizophrenia-like symptoms induced in mice via administration of subanesthetic doses of ketamine are alleviated by trodusquemine [84]. Mechanistically, PTP1B ablation in glutamatergic neurons seems to mediate ketamine-induced deficits in endocannabinoid mobilization, memory and sensorimotor gating. This study and our results herein emphasize the potential benefit of targeting PTP1B to prevent metabolic comorbidities in patients under OLA treatment, as well as to ameliorate schizophrenia-like symptoms.

Browning of iWAT has arisen as a contributor to whole-body energy balance [85]. Our results revealed that, in both WT and PTP1B-deficient male mice, i.p. OLA administration reduced lipid droplet size and elevated UCP-1 in iWAT, histological features of browning. This effect was associated with an increase in TH positive sympathetic innervation, which controls adipose tissue function [86,87], as well as less number of SAMs. These macrophages were recently proposed as responsible for clearing the excess of noradrenaline upon stimulation of the sympathetic fibers [87]. These results, together with increased iWAT UCP-1 and TH levels in mice receiving an intrahypothalamic OLA injection, and the failure of OLA in inducing these changes in explants from mice and humans, strongly support hypothalamic signals via sympathetic nervous system as mediators of OLA actions in iWAT upon i.p. administration. These results are reinforced by our previous ex vivo studies in human WAT explants describing the inability of SGAs to alter the expression of adipokines or genes involved in energy regulation [42,88]. Moreover, the hypothalamic-iWAT connection by OLA leading to browning

paralleled with a reduction of hypothalamic phospho-AMPK in agreement with the work of Martins et al. on the effect of BMP8b on energy balance [49]. Furthermore, the prevention of OLA-mediated UCP-1 elevation by AMPKα1 activation in the hypothalamus reinforces the negative modulation of AMPK in this brain region as inducer of iWAT browning by this SGA. In this line, the effect of leptin in increasing WAT lipolysis has been recently attributed to the actions of sympathetic neuronal efferents to adipose tissue [86], supporting the neuro-adipose junction in WAT. Interestingly, neither WT nor PTP1B-KO mice treated orally with OLA presented changes in iWAT UCP-1 levels, emphasizing the potential therapeutic advantage of an injectable treatment when compared to the oral administration.

The translational value of our results is supported by the recent findings on the relevance of activation of BAT and/or browning of WAT in humans by cold exposure or drug interventions to target obesity, as reviewed [89,90]. Also of clinical relevance, a recent study has reported safety of intravenous OLA administration in patients even after multiple doses [91]. In another study, individuals with schizophrenia were followed-up during 24 weeks of treatment with OLA either orally (10, 15, or 20 mg/day) or by injections of a long-acting formulation (150 mg every 2 weeks, 405 mg every 4 weeks, or 300 mg every 2 weeks) [92]. Despite both groups presented a significantly increase in the mean body weight, the group under long-acting OLA injection gained less weight, although not significantly differences were found. Importantly, patients who were obese at the beginning of the treatment showed a significant lower weight gain when treated with long-acting OLA injection than the obese patients receiving oral OLA treatment. Moreover, a 6-year clinical study of the efficacy and safety of the OLA long-acting injection in patients with schizophrenia showed that these patients had a mean increase of their body weight of 2.1–2.2 kg after the treatment period [93,94]. Although this study was not conducted in parallel in patients under oral treatment, a meta-analysis of 78 studies showed a weight gain of 4.15 kg during 10 weeks of OLA oral treatment [95]. These promising studies support the potential therapeutic value of our preclinical study based on implementation of an OLA i.p. treatment.

Finally, the impact of gut microbiota in the oral treatment with OLA must also be taken into account since contradictory results have been reported. For instance, rats treated orally with OLA reshape their gut microbiota in a very similar way that high fat-diet does [25,96], resulting in a worse prognosis of weight gain. On the other hand, a 10-day study in healthy men showed that OLA does not alter the plasma concentration of gut hormones [97]. Other study reported that patients treated with OLA for 6 months have increased ghrelin and leptin plasma levels, as well as adiposity [98]. Moreover, plasma ghrelin was the only gut hormone found elevated in male rats orally treated with OLA [99], supporting the underlie impairment in satiation by OLA administered orally. Altogether, these studies point dysbiosis and/or changes in ghrelin secretion as possible additional factors by which oral treatments with OLA can lead to weight gain. Moreover, gut microbiota, which is modulated by many factors, can also influence plasma and, hence, hypothalamic OLA availability in oral treatments.

Overall, our results suggest that, based on the administration route, OLA modulates energy balance in AMPK dependent- or independent manner. Whereas reduction of hypothalamic phospho-AMPK increases EE, as proven by OLA administration via i.p, the decrease of EE in the dietary treatment occurs in a hypothalamic-AMPK independent-manner. Taking into account the substantial differences in OLA levels reaching this brain region in mice receiving a single i.p. injection compared to a single oral administration, our data strongly suggest that to avoid weight gain through the activation of the hypothalamus-BAT/iWAT axis a threshold of OLA level in the hypothalamus is required which is achieved by the i.p. administration and not by the oral treatment in which drug absorption is influenced by multiple factors.

5. Conclusion

This study has revealed an interactome between the hypothalamus and BAT/iWAT in response to an OLA i.p treatment, pointing this hypothalamic AMPK-driven crosstalk as responsible for BAT and iWAT activation. This complex metabolic rewiring was associated with higher hypothalamic OLA levels and body weight loss when male mice were treated with OLA via i.p. These results, together with the protection against OLA-induced weight gain conferred by PTP1B deficiency in the oral treatment, might have translational implications to avoid obesity and other associated metabolic side effects of OLA.

Supplementary data to this article can be found online at https://doi.org/10.1016/j.metabol.2022.155335.

CRediT authorship contribution statement

The study was designed by VF, PR and ÁMV. Mice treatments, data acquisition, analysis and interpretation were performed by VF, PR and ÁMV. Immunohistochemistry and immunofluorescence analyses were performed by VF. Protein expression analysis was performed by VF, PR and ÁMV. Central injections were performed by VF, MG and PLL. Central adenoviral injections and posterior treatment with OLA were done by VF, CF and GS. Concentrations of OLA in plasma were determined by MN, PZ and FAS and analyzed by VF. Human explants experiments were done by AS, MJP and JWE. VF, PR and ÁMV wrote the first draft of the manuscript. CF, MG, MN, PZ, AS, PLL, JWE, MJP, FAS and GS critically revised the manuscript for important intellectual content. All authors gave final approval of the manuscript and gave consent to its publication. ÁMV and PR coordinated the study and ÁMV is the guarantor of the work.

Declaration of competing interest

The authors declare no conflict of interest. Also, the authors declare that there are no relationships or activities that might bias, or be perceived to bias, their work.

Data availability

Data presented in this manuscript are available upon request from the corresponding authors.

Acknowledgements

References

[1] Rosen WG, et al. Positive and negative symptoms in schizophrenia. Psychiatry Res. 1984;13(4):277–84.

[2] Remington G, et al. Guidelines for the pharmacotherapy of schizophrenia in adults. Can. J. Psychiatry 2017;62(9):604–16. https://doi.org/10.1177/0706743717720448.

[3] Cohen D, et al. Hyperglycemia and diabetes in patients with schizophrenia or schizoaffective disorders. Diabetes Care 2006;29(4):786–91.

[4] Kurzthaler I, Fleischhacker WW. The clinical implications of weight gain in schizophrenia. J. Clin. Psychiatry. 2001;62(Suppl 7):32–7.

[5] Grajales D, Ferreira V, Valverde AM. Second-generation antipsychotics and dysregulation of glucose metabolism: beyond weight gain. Cells 2019;8(11). https://doi.org/10.3390/cells8111336.

[6] Burghardt KJ, et al. Atypical antipsychotics, insulin resistance and weight; a meta-analysis of healthy volunteer studies. Prog Neuropsychopharmacol Biol Psychiatry 2018;83:55–63. https://doi.org/10.1016/j.pnpbp.2018.01.004.

[7] Leucht S, et al. Comparative efficacy and tolerability of 15 antipsychotic drugs in schizophrenia: a multiple-treatments meta-analysis. Lancet 2013;382(9896): 951–62. https://doi.org/10.1016/S0140-6736(13)60733-3.

[8] Lochmann van Bennekom MW, Gijsman HJ, Zitman FG. Antipsychotic polypharmacy in psychotic disorders: a critical review of neurobiology, efficacy, tolerability and cost effectiveness. J Psychopharmacol 2013;27(4):327–36. https://doi.org/10.1177/0269881113477709.

[9] Ferreira V, Grajales D, Valverde AM. Adipose tissue as a target for second-generation (atypical) antipsychotics: a molecular view. Biochim. Biophys. Acta. Mol. Cell Biol. Lipids 2020;1865(2):158534. https://doi.org/10.1016/j.bbalip.2019.158534.

[10] Albaugh VL, et al. Hormonal and metabolic effects of olanzapine and clozapine related to body weight in rodents. Obesity (Silver Spring) 2006;14(1):36–51. https://doi.org/10.1038/oby.2006.6.

[11] Zhang Q, et al. Olanzapine reduced brown adipose tissue thermogenesis and locomotor activity in female rats. Prog. Neuropsychopharmacol. Biol. Psychiatry. 2014;51:172–80. https://doi.org/10.1016/j.pnpbp.2014.02.003.

[12] Fedorenko A, Lishko PV, Kirichok Y. Mechanism of fatty-acid-dependent UCP1 uncoupling in brown fat mitochondria. Cell 2012;151(2):400–13. https://doi.org/10.1016/j.cell.2012.09.010.

[13] Morrison SF, Madden CJ, Tupone D. Central neural regulation of brown adipose tissue thermogenesis and energy expenditure. Cell Metab. 2014;19(5):741–56. https://doi.org/10.1016/j.cmet.2014.02.007.

[14] Zingaretti MC, et al. The presence of UCP1 demonstrates that metabolically active adipose tissue in the neck of adult humans truly represents brown adipose tissue. FASEB J. 2009;23(9):3113–20. https://doi.org/10.1096/fj.09-133546.

[15] Kajimura S, Spiegelman BM, Seale P. Brown and Beige fat: physiological roles beyond heat generation. Cell Metab. 2015;22(4):546–59. https://doi.org/10.1016/j.cmet.2015.09.007.

[16] Gonzalez-Rodriguez A, et al. Essential role of protein tyrosine phosphatase 1B in obesity-induced inflammation and peripheral insulin resistance during aging. Aging Cell 2012;11(2):284–96. https://doi.org/10.1111/j.1474-9726.2011.00786.x.

[17] Gonzalez-Rodriguez A, et al. Resveratrol treatment restores peripheral insulin sensitivity in diabetic mice in a sirt1-independent manner. Mol. Nutr. Food. Res. 2015;59(8):1431–42. https://doi.org/10.1002/mnfr.201400933.

[18] Delibegovic M, et al. Liver-specific deletion of protein-tyrosine phosphatase 1B (PTP1B) improves metabolic syndrome and attenuates diet-induced endoplasmic reticulum stress. Diabetes 2009;58(3):590–9. https://doi.org/10.2337/db08-0913.

[19] Fountaine RJ, et al. Increased food intake and energy expenditure following administration of olanzapine to healthy men. Obesity (Silver Spring) 2010;18(8): 1646–51. https://doi.org/10.1038/oby.2010.6.

[20] Chen VC, et al. Leptin/Adiponectin ratio as a potential biomarker for metabolic syndrome in patients with schizophrenia. Psychoneuroendocrinology 2018;92: 34–40. https://doi.org/10.1016/j.psyneuen.2018.03.021.

[21] Razavi BM, et al. Carnosic acid prevented olanzapine-induced metabolic disorders through AMPK activation. Mol. Biol. Rep. 2020;47(10):7583–92. https://doi.org/10.1007/s11033-020-05825-5.

[22] Garcia-Ruiz I, et al. Protein tyrosine phosphatase 1b deficiency protects against hepatic fibrosis by modulating nadph oxidases. Redox Biol. 2019;26:101263. https://doi.org/10.1016/j.redox.2019.101263.

[23] Grajales D, et al. The second-generation antipsychotic drug aripiprazole modulates the serotonergic system in pancreatic islets and induces beta cell dysfunction in female mice. Diabetologia 2022;65(3):490–505. https://doi.org/10.1007/s00125-021-05630-0.

[24] Ardic CM, et al. Olanzapine induced reproductive toxicity in male rats. Sci. Rep. 2021;11(1):4739. https://doi.org/10.1038/s41598-021-84235-4.

[25] Morgan AP, et al. The antipsychotic olanzapine interacts with the gut microbiome to cause weight gain in mouse. PLoS One 2014;9(12):e115225. https://doi.org/10.1371/journal.pone.0115225.

[26] Savoy YE, et al. Differential effects of various typical and atypical antipsychotics on plasma glucose and insulin levels in the mouse: evidence for the involvement of sympathetic regulation. Schizophr. Bull. 2010;36(2):410–8. https://doi.org/10.1093/schbul/sbn104.

[27] Boyda HN, et al. A parametric study of the acute effects of antipsychotic drugs on glucose sensitivity in an animal model. Prog. Neuropsychopharmacol. Biol. Psychiatry 2010;34(6):945–54. https://doi.org/10.1016/j.pnpbp.2010.04.024.

[28] Boyda HN, et al. Routine exercise ameliorates the metabolic side-effects of treatment with the atypical antipsychotic drug olanzapine in rats. Int. J. Neu 2014; 17(1):77–90. https://doi.org/10.1017/S1461145713000795.

[29] Mondelli V, et al. Haloperidol and olanzapine mediate metabolic abnormalities through different molecular pathways. Transl. Psychiatry 2013;3:e208. https://doi.org/10.1038/tp.2012.138.

[30] Calevro A, et al. Effects of chronic antipsychotic drug exposure on the expression of translocator protein and inflammatory markers in rat adipose tissue. Psychoneuroendocrinology 2018;95:28–33. https://doi.org/10.1016/j.psyneuen.2018.05.021.

[31] Assie MB, et al. The antipsychotics clozapine and olanzapine increase plasma glucose and corticosterone levels in rats: comparison with aripiprazole, ziprasidone, bifeprunox and F15063. Eur. J. Pharmacol. 2008;592(1–3):160–6. https://doi.org/10.1016/j.ejphar.2008.06.105.

[32] Waldman L, et al. Chronic oral olanzapine treatment but not haloperidol decreases [(3)H] MK-801 binding in the rat brain independent of dietary conditions. Neurosci. Lett. 2022;781:136657. https://doi.org/10.1016/j.neulet.2022.136657.

[33] Terry Jr AV, et al. Negative effects of chronic oral chlorpromazine and olanzapine treatment on the performance of tasks designed to assess spatial learning and working memory in rats. Neuroscience 2008;156(4):1005–16. https://doi.org/10.1016/j.neuroscience.2008.08.030.

[34] Terry Jr AV, et al. Differential effects of chronic haloperidol and olanzapine exposure on brain cholinergic markers and spatial learning in rats. Psychopharmacology (Berl) 2002;164(4):360–8. https://doi.org/10.1007/s00213-002-1230-z.

[35] Ikegami M, et al. Olanzapine-induced hyperglycemia: possible involvement of histaminergic, dopaminergic and adrenergic functions in the central nervous system. Neuroendocrinology 2013;98(3):224–32. https://doi.org/10.1159/000356119.

[36] Franklin KBJ, Paxinos G. Paxinos and Franklin's The Mouse Brain in Stereotaxic Coordinates. Fourth edition. Amsterdam: Academic Press; 2013. an imprint of Elsevier. 1 volume (unpaged).

[37] Lopez M, et al. Hypothalamic AMPK and fatty acid metabolism mediate thyroid regulation of energy balance. Nat. Med. 2010;16(9):1001–8. https://doi.org/10.1038/nm.2207.

[38] Martinez de Morentin PB, et al. Estradiol regulates brown adipose tissue thermogenesis via hypothalamic AMPK. Cell Metab. 2014;20(1):41–53. https://doi.org/10.1016/j.cmet.2014.03.031.

[39] Martinez-Sanchez N, et al. Hypothalamic AMPK-ER Stress-JNK1 Axis Mediates the Central Actions of Thyroid Hormones on Energy Balance. Cell Metab 2017;26(1): 212–29. https://doi.org/10.1016/j.cmet.2017.06.014. e12.

[40] Garcia-Casarrubios E, et al. Rapamycin negatively impacts insulin signaling, glucose uptake and uncoupling protein-1 in brown adipocytes. Biochim. Biophys. Acta 2016;1861(12 Pt A):1929–41. https://doi.org/10.1016/j.bbalip.2016.09.016.

[41] Mellon PL, et al. Immortalization of hypothalamic GnRH neurons by genetically targeted tumorigenesis. Neuron 1990;5(1):1–10. https://doi.org/10.1016/0896-6273(90)90028-e.

[42] Sarsenbayeva A, et al. Effects of second-generation antipsychotics on human subcutaneous adipose tissue metabolism. Psychoneuroendocrinology 2019;110: 104445. https://doi.org/10.1016/j.psyneuen.2019.104445.

[43] Muller TD, Klingenspor M, Tschop MH. Revisiting energy expenditure: how to correct mouse metabolic rate for body mass. Nat. Metab. 2021;3(9):1134–6. https://doi.org/10.1038/s42255-021-00451-2.

[44] Saenz de Urturi D, et al. Methionine adenosyltransferase 1a antisense oligonucleotides activate the liver-brown adipose tissue axis preventing obesity and associated hepatosteatosis. Nat. Commun. 2022;13(1):1096. https://doi.org/10.1038/s41467-022-28749-z.

[45] Nagashima K. Central mechanisms for thermoregulation in a hot environment. Ind. Health 2006;44(3):359–67. https://doi.org/10.2486/indhealth.44.359.

[46] Seoane-Collazo P, et al. Activation of hypothalamic AMP-activated protein kinase ameliorates metabolic complications of experimental arthritis. Arthritis Rheumatol. 2022;74(2):212–22. https://doi.org/10.1002/art.41950.

[47] Prior TI, Baker GB. Interactions between the cytochrome P450 system and the second-generation antipsychotics. J. Psychiatry. Neurosci. 2003;28(2):99–112.

[48] Kim SH, Plutzky J. Brown fat and Browning for the treatment of obesity and related metabolic disorders. Diabetes Metab. J. 2016;40(1):12–21. https://doi.org/10.4093/dmj.2016.40.1.12.

[49] Martins L, et al. A functional link between AMPK and orexin mediates the effect of BMP8B on energy balance. Cell Rep. 2016;16(8):2231–42. https://doi.org/10.1016/j.celrep.2016.07.045.

[50] Jain S, Bhargava M, Gautam S. Weight gain with olanzapine: drug, gender or age? Indian J Psychiatry 2006;48(1):39–42. https://doi.org/10.4103/0019-5545.31617.

[51] Terry Jr AV, et al. Chronic exposure to typical or atypical antipsychotics in rodents: temporal effects on central alpha7 nicotinic acetylcholine receptors. Neuroscience 2005;136(2):519–29. https://doi.org/10.1016/j.neuroscience.2005.08.006.

[52] Lopez M. Hypothalamic AMPK and energy balance. Eur. J. Clin. Invest. 2018;48(9): e12996. https://doi.org/10.1111/eci.12996.

[53] Heras V, et al. Central Ceramide Signaling Mediates Obesity-Induced Precocious Puberty. Cell Metab 2020;32(6):951–66. https://doi.org/10.1016/j. cmet.2020.10.001. e8.

[54] Capelli V, et al. Orally induced hyperthyroidism regulates hypothalamic AMP-activated protein kinase. Nutrients 2021;13(12). https://doi.org/10.3390/ nu13124204.

[55] Lopez M. Estrogen wars: the activity awakens. Cell Metab. 2021;33(12):2309–11. https://doi.org/10.1016/j.cmet.2021.11.006.

[56] Milbank E, et al. Small extracellular vesicle-mediated targeting of hypothalamic AMPKalpha1 corrects obesity through BAT activation. Nat. Metab. 2021;3(10): 1415–31. https://doi.org/10.1038/s42255-021-00467-8.

[57] Lopez M, et al. Hypothalamic AMPK: a canonical regulator of whole-body energy balance. Nat. Rev. Endocrinol. 2016;12(7):421–32. https://doi.org/10.1038/ nrendo.2016.67.

[58] Escalona-Garrido C, et al. Moderate SIRT1 overexpression protects against brown adipose tissue inflammation. Mol Metab 2020;42:101097. https://doi.org/ 10.1016/j.molmet.2020.101097.

[59] Chen X, et al. Olanzapine increases AMPK-NPY orexigenic signaling by disrupting H1R-GHSR1a interaction in the hypothalamic neurons of mice. Psychoneuroendocrinology 2020;114:104594. https://doi.org/10.1016/j. psyneuen.2020.104594.

[60] Kageyama H, et al. Neuronal circuits involving neuropeptide Y in hypothalamic arcuate nucleus-mediated feeding regulation. Neuropeptides 2012;46(6):285–9. https://doi.org/10.1016/j.npep.2012.09.007.

[61] Rondini TA, et al. Hypothalamic cocaine- and amphetamine-regulated transcript neurons project to areas expressing gonadotropin releasing hormone immunoreactivity and to the anteroventral periventricular nucleus in male and female rats. Neuroscience 2004;125(3):735–48. https://doi.org/10.1016/j. neuroscience.2003.12.045.

[62] Lopez M. Hypothalamic AMPK as a possible target for energy balance-related diseases. Trends Pharmacol. Sci. 2022;43(7):546–56. https://doi.org/10.1016/j. tips.2022.04.007.

[63] Skrede S, et al. Olanzapine depot formulation in rat: a step forward in modelling antipsychotic-induced metabolic adverse effects. Int. J. Neuropsychiatry 2014;17 (1):91–104. https://doi.org/10.1017/S1461145713000862.

[64] Ferno J, et al. Olanzapine-induced hyperphagia and weight gain associate with orexigenic hypothalamic neuropeptide signaling without concomitant AMPK phosphorylation. PLoS One 2011;6(6):e20571. https://doi.org/10.1371/journal. pone.0020571.

[65] He M, et al. Hypothalamic histamine H1 receptor-AMPK signaling time-dependently mediates olanzapine-induced hyperphagia and weight gain in female rats. Psychoneuroendocrinology 2014;42:153–64. https://doi.org/10.1016/j. psyneuen.2014.01.018.

[66] Skrede S, et al. Lack of ovarian secretions reverts the anabolic action of olanzapine in female rats. Int. J. Neuropsychopharmacol. 2017;20(12):1005–12. https://doi. org/10.1093/ijnp/pyx073.

[67] Ferno J, et al. Olanzapine depot exposure in male rats: dose-dependent lipogenic effects without concomitant weight gain. Eur. Neurol. 2015;25(6):923–32. https:// doi.org/10.1016/j.euroneuro.2015.03.002.

[68] Gao Q, Horvath TL. Neuronal control of energy homeostasis. FEBS Lett. 2008;582 (1):132–41. https://doi.org/10.1016/j.febslet.2007.11.063.

[69] Cone RD, et al. The arcuate nucleus as a conduit for diverse signals relevant to energy homeostasis. Int. J. Obes. Relat. Metab. Disord. 2001;25(Suppl 5):S63–7. https://doi.org/10.1038/sj.ijo.0801913.

[70] Ruffin M, Nicolaidis S. Electrical stimulation of the ventromedial hypothalamus enhances both fat utilization and metabolic rate that precede and parallel the inhibition of feeding behavior. Brain. Res. 1999;846(1):23–9. https://doi.org/ 10.1016/s0006-8993(99)01922-8.

[71] Zhang J, et al. An excitatory ventromedial hypothalamus to paraventricular thalamus circuit that suppresses food intake. Nat. Commun. 2020;11(1):6326. https://doi.org/10.1038/s41467-020-20093-4.

[72] Sternson SM, Shepherd GM, Friedman JM. Topographic mapping of VMH –> arcuate nucleus microcircuits and their reorganization by fasting. Nat. Neurosci. 2005;8(10):1356–63. https://doi.org/10.1038/nn1550.

[73] Wu RR, et al. Metformin treatment of antipsychotic-induced dyslipidemia: an analysis of two randomized, placebo-controlled trials. Mol. Psychiatry 2016;21 (11):1537–44. https://doi.org/10.1038/mp.2015.221.

[74] Chau-Van C, et al. Metformin inhibits adenosine 5'-monophosphate-activated kinase activation and prevents increases in neuropeptide Y expression in cultured hypothalamic neurons. Endocrinology 2007;148(2):507–11. https://doi.org/ 10.1210/en.2006-1237.

[75] Stevanovic D, et al. Intracerebroventricular administration of metformin inhibits ghrelin-induced hypothalamic AMP-kinase signalling and food intake. Neuroendocrinology 2012;96(1):24–31. https://doi.org/10.1159/000333963.

[76] Lee CK, et al. Intracerebroventricular injection of metformin induces anorexia in rats. Diabetes Metab. J. 2012;36(4):293–9. https://doi.org/10.4093/ dmj.2012.36.4.293.

[77] Pescador N, et al. Metformin reduces macrophage HIF1alpha-dependent proinflammatory signaling to restore brown adipocyte function in vitro. Redox Biol. 2021;48:102171. https://doi.org/10.1016/j.redox.2021.102171.

[78] Rubio C, et al. Impact of global PTP1B deficiency on the gut barrier permeability during NASH in mice. Mol Metab 2020;35:100954. https://doi.org/10.1016/j. molmet.2020.01.018.

[79] Gonzalez-Rodriguez A, et al. Dual role of protein tyrosine phosphatase 1B in the progression and reversion of non-alcoholic steatohepatitis. Mol Metab 2018;7: 132–46. https://doi.org/10.1016/j.molmet.2017.10.008.

[80] Arroba AI, Valverde AM. Inhibition of protein tyrosine phosphatase 1B improves IGF-I receptor signaling and protects against inflammation-induced gliosis in the retina. Invest. Ophthalmol. Vis. Sci. 2015;56(13):8031–44. https://doi.org/ 10.1167/iovs.15-17234.

[81] Xue B, et al. Neuronal protein tyrosine phosphatase 1B deficiency results in inhibition of hypothalamic AMPK and isoform-specific activation of AMPK in peripheral tissues. Mol. Cell. Biol. 2009;29(16):4563–73. https://doi.org/10.1128/ MCB.01914-08.

[82] Tsou RC, et al. Improved metabolic phenotype of hypothalamic PTP1B-deficiency is dependent upon the leptin receptor. Mol Metab 2014;3(3):301–12. https://doi. org/10.1016/j.molmet.2014.01.008.

[83] Miranda S, et al. Beneficial effects of PTP1B deficiency on brown adipocyte differentiation and protection against apoptosis induced by pro- and anti-inflammatory stimuli. Cell. Signal. 2010;22(4):645–59. https://doi.org/10.1016/j. cellsig.2009.11.019.

[84] Qin Z, et al. Ketamine's schizophrenia-like effects are prevented by targeting PTP1B. Neurobiol. Dis. 2021;155:105397. https://doi.org/10.1016/j. nbd.2021.105397.

[85] Wu J, Cohen P, Spiegelman BM. Adaptive thermogenesis in adipocytes: is beige the new brown? Genes Dev. 2013;27(3):234–50. https://doi.org/10.1101/ gad.211649.112.

[86] Zeng W, et al. Sympathetic neuro-adipose connections mediate leptin-driven lipolysis. Cell 2015;163(1):84–94. https://doi.org/10.1016/j.cell.2015.08.055.

[87] Pirzgalska RM, et al. Sympathetic neuron-associated macrophages contribute to obesity by importing and metabolizing norepinephrine. Nat. Med. 2017;23(11): 1309–18. https://doi.org/10.1038/nm.4422.

[88] Sarsenbayeva A, et al. Human macrophages stimulate expression of inflammatory mediators in adipocytes; effects of second-generation antipsychotics and glucocorticoids on cellular cross-talk. Psychoneuroendocrinology 2021;125: 105071. https://doi.org/10.1016/j.psyneuen.2020.105071.

[89] Finlin BS, et al. Human adipose beiging in response to cold and mirabegron. JCI Insight 2018;3(15). https://doi.org/10.1172/jci.insight.121510.

[90] Carobbio S, et al. Brown and beige fat: from molecules to physiology and pathophysiology. Biochim. Biophys. Acta Mol. Cell Biol. Lipids 2019;1864(1): 37–50. https://doi.org/10.1016/j.bbalip.2018.05.013.

[91] Hunt NF, et al. Safety of intravenous olanzapine administration at a Tertiary Academic Medical Center. Ann. Pharmacother. 2021;55(9):1127–33. https://doi. org/10.1177/1060028020988734.

[92] McDonnell DP, et al. Comparison of metabolic changes in patients with schizophrenia during randomized treatment with intramuscular olanzapine long-acting injection versus oral olanzapine. Hum. Psychol. 2011;26(6):422–33. https://doi.org/10.1002/hup.1225.

[93] McDonnell DP, Landry J, Detke HC. Long-term safety and efficacy of olanzapine long-acting injection in patients with schizophrenia or schizoaffective disorder: a 6-year, multinational, single-arm, open-label study. Int. Clin. Psychopharmacol. 2014;29(6):322–31. https://doi.org/10.1097/YIC.0000000000000038.

[94] Anand E, et al. A 6-year open-label study of the efficacy and safety of olanzapine long-acting injection in patients with schizophrenia: a post hoc analysis based on the european label recommendation. Neuropsychiatr. Dis. Treat. 2015;11: 1349–57. https://doi.org/10.2147/NDT.S79347.

[95] Allison DB, et al. Antipsychotic-induced weight gain: a comprehensive research synthesis. Am. J. Psychiatry. 1999;156(11):1686–96. https://doi.org/10.1176/ ajp.156.11.1686.

[96] Davey KJ, et al. Antipsychotics and the gut microbiome: olanzapine-induced metabolic dysfunction is attenuated by antibiotic administration in the rat. Transl. Psychiatry 2013;3:e309. https://doi.org/10.1038/tp.2013.83.

[97] Vidarsdottir S, et al. Short-term treatment with olanzapine does not modulate gut hormone secretion: olanzapine disintegrating versus standard tablets. Eur. J. Endocrinol. 2010;162(1):75–83. https://doi.org/10.1530/EJE-09-0433.

[98] Murashita M, et al. Olanzapine increases plasma ghrelin level in patients with schizophrenia. Psychoneuroendocrinology 2005;30(1):106–10. https://doi.org/ 10.1016/j.psyneuen.2004.05.008.

[99] van der Zwaal EM, et al. The acute effects of olanzapine on ghrelin secretion, CCK sensitivity, meal size, locomotor activity and body temperature. Int. J. Obes. (Lond) 2012;36(2):254–61. https://doi.org/10.1038/ijo.2011.97.